

Multi-Robot Multi-Room Exploration with Geometric Cue Extraction and Spherical Decomposition

Seungchan Kim¹, Micah Corah¹, John Keller¹, Graeme Best², Sebastian Scherer¹

Abstract—This work proposes an autonomous multi-robot exploration pipeline that coordinates the behaviors of robots in an indoor environment composed of multiple rooms. Contrary to simple frontier-based exploration approaches, we aim to enable robots to methodically explore and observe an unknown set of rooms in a structured building, keeping track of which rooms are already explored and sharing this information among robots to coordinate their behaviors in a distributed manner. To this end, we propose (1) a geometric cue extraction method that processes 3D map point cloud data and detects the locations of potential cues such as doors and rooms, (2) a spherical decomposition for open spaces used for target assignment. Using these two components, our pipeline effectively assigns tasks among robots, and enables a methodical exploration of rooms. We evaluate the performance of our pipeline using a team of up to 3 aerial robots, and show that our method outperforms the baseline by 36.6% in simulation and 26.4% in real-world experiments. (Video link: <https://youtu.be/wRLEY4FHZko>)

I. INTRODUCTION

Multi-robot exploration [1, 2] in unfamiliar, unknown environments has attracted attention in the robotics research community, due to its potential to accomplish duties faster than a single robot, and its wide applicability in tasks including search & rescue operations [3], hazardous source detection in turbulent environments [4], and planetary missions [5]. Recently, in light of the DARPA Subterranean Challenge, there is a growing attention on exploration of large underground and indoor environments by teams of robots, with realistic communication constraints, sensor coverage, and compute conditions [6–8]. In this work, we aim to develop a more structured multi-robot autonomous exploration pipeline for operation in indoor environments, taking advantage of geometric properties of structures in a building.

Specifically, we aim to build algorithms for multiple robots exploring inside a building composed of multiple rooms, whose locations and sizes are not known in advance. Rather than following a frontier-based approach [9], we explicitly model the geometry of rooms to enable a methodical exploration of structural environments, empowering robots to explore the rooms one by one, observing each room in turn before moving on to another. Furthermore, we also want coordinated behaviors such that robots select rooms to avoid redundant observations by multiple robots, and we

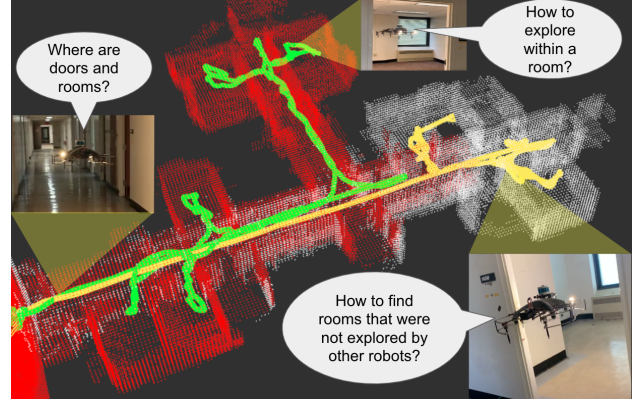


Fig. 1. We present an autonomous multi-robot exploration pipeline that coordinates the behaviors of robots exploring multiple rooms in a building. Using our pipeline, robots explore different rooms in a methodical manner. The traveled trajectory and area covered by each robot is visualized with different color.

are interested in performing detailed observation of these confined spaces (rooms) with a primary sensor, such as an RGB camera, at close range [10].

Why do we want this type of multi-room exploration? First, rooms are usually the parts of the building where meaningful target objects are placed in, compared to corridors and hallways. Thus, they warrant focused attention during exploration. Second, rooms are non-overlapping and structural units that constitute the building; the entire indoor space can be segmented using a room-oriented search. One thing to consider is that, when we deploy multiple robots for room-oriented search, it is inefficient to assign multiple robots to the same small room; thus, we need a coordinated target assignment scheme for multi-robot, multi-room exploration.

To this end, we propose our method, Multi-Robot Multi-Room (MRMR). Unlike learning-based geometry prediction for exploration, our method does not require an offline dataset for representative environments to learn from. Instead, we use a simple yet effective and generalizable technique to extract geometric cues that indicate the potential locations of doors and rooms, only from 3D point cloud LiDAR data. Our pipeline processes map data observed by LiDAR sensors onboard, converting 3D point cloud voxels into a 2D binary image, and then into a 2D distance transform map. Using the 2D distance transform map, robots perform real-time geometric analysis to discover structural cues that signal the doors and rooms. Robots update global plans and execute local planners accordingly, actively searching for unreached doors and unexplored rooms in the space.

¹ S. Kim, M. Corah, J. Keller, and S. Scherer are with Robotics Institute, Carnegie Mellon University, Pittsburgh, PA 15213, USA. {seungch2, micahc, jkeller2, basti}@andrew.cmu.edu

² G. Best is with School of Mechanical and Mechatronic Engineering, University of Technology Sydney, Ultimo NSW 2007, Australia. graeme.best@uts.edu.au

This work is supported by Defense Science and Technology Agency Singapore.

We also propose the idea of representing the confined spaces (e.g. rooms) with spheres. We show that spherical decomposition is a compact representation of the environment for robots exploring rooms and sharing necessary information with other robots via communication.

We evaluate our autonomous exploration pipeline using multiple unmanned aerial vehicles (UAV), both in simulation and real-world experiments. Built upon the multi-robot exploration and planning component of the complete autonomy stack [10] of Team Explorer, which showed most successful exploration by aerial robots in the final round of DARPA SubT Challenge competition, our methods record significant performance gain in fast discovery and exploration of multiple rooms, and coordination of behaviors for multiple robots.

In summary, our contributions are:

- An autonomous multi-robot exploration pipeline that coordinates behaviors of robots in a building composed of multiple rooms.
- Incorporation of two new modules for multi-robot multi-room exploration: (1) a geometric cue extraction method that detects the locations of doors and rooms from 3D LiDAR point cloud data, and (2) spherical decomposition of spaces for room representation, target assignments, and communication.
- Empirical validation of our multi-robot exploration pipeline via simulated and real-world experiments.

II. RELATED WORK

A. Multi-robot Exploration

Multi-robot exploration problems have been studied with various approaches. Many prior works [1, 9] view this problem as an assignment of frontiers (the boundaries between known and unknown space), where robots explore environments by continuously moving toward nearby, unexplored frontiers. Other approaches include sampling-based [11], information-theoretic [12, 13], graph search-based [14], recursive tree-based search [15], and sub-map merging [16]. Recent works include hybrid approaches, such as combining frontier-based approach and graph-search [10].

Multi-robot exploration research can also be categorized by whether decision-making is centralized or decentralized. In centralized schemes [17, 18], a central entity plans out tasks for a team of robots with an access to the global information of the environment, which could hypothetically produce globally optimal solutions. However, a single failure of a robot or communication link could lead to the failure of the entire system. Instead, we follow the decentralized [19, 20] schemes, which are more robust to the single point of failure. Each robot makes decisions and optimizes trajectories based on its own understanding of the environment, with realistic communication constraints among robots.

B. Space Partitioning and Decomposition

In robotic exploration research, space partitioning approaches decompose space into subparts or partitions and seek to cover the whole space by consecutively exploring the partitions. Wu et al. [21] proposes Voronoi-based partitioning

to coordinate multi-robot exploration, dividing the entire space into a set of polygons. Solanas and Garcia [22] propose using unsupervised clustering for multi-robot coordination. Hu et al. [23] uses the combination of deep reinforcement learning and Voronoi-based partitions to improve coordination strategies for multi-robot exploration.

C. Room Detection

Division of a floorplan into rooms, or identifying the potential location and size of rooms is essential to room-based search and exploration. Most popular approach to detect rooms is Voronoi-based approach by Thrun [24], which utilizes distance transform and Voronoi graph to find critical points in the map to detect passages to the room. Wurm et al. [25] uses this idea to divide the space map into segments that can correspond to individual rooms, and generate Voronoi graph to assign targets for each robot in the multi-robot teams, in a centralized manner.

Other works include graph-based partitioning which uses topological map to cluster nodes and build higher-level hierarchical map [26], or feature-based room segmentation approaches [27] which learns features and geometric shapes that match with the characteristic of rooms. More recently, Rosinol et al. [28] proposed 3D dynamics scene graph, with multiple layers in the hierarchy representing different levels of semantic structures, where rooms are composed using lower-level layer graph nodes like walls, floors, and ceiling.

In this work, we focus on LiDAR processing approach that enables high-speed, low-compute processing onboard and robust exploration in light-degraded environments, as opposed to learning-based approaches that often require a large amount of computations and pretraining of offline datasets. We revisit the idea of distance transform map [24], but improve this idea by using a different cue detection method and space decompositions that are compatible with state-of-the-art fully autonomous multi-robot exploration algorithms.

III. PROBLEM DEFINITION

Consider a team of n robots ($i = 1, 2, \dots, n$) that are exploring an indoor environment. Denote the trajectory traveled by each robot as ξ_i . The robots build a map of the environment with LiDAR, which is represented with a 3D occupancy voxel grid in a shared coordinate system (each voxel represents a cube with side length 0.2m). The robots observe surfaces of the environment with a primary sensor, such as a camera or RGBD sensor with limited field of view. The intersection between the occupied voxels of the LiDAR map and the primary sensor field of view is denoted by the voxel grid O_i (for robot i). The observation model for the primary sensor can be defined based on the specifications of the robot and the application; we model the primary sensor as a forward-facing fish-eye camera with a 5m field of view, modelling occlusions with ray casting, as in [10].

Let us assume that there are total K rooms to be explored in the building, and denote V_j^{rm} ($j = 1, 2, \dots, K$) as voxels within each room. Then, the total number of voxels in these

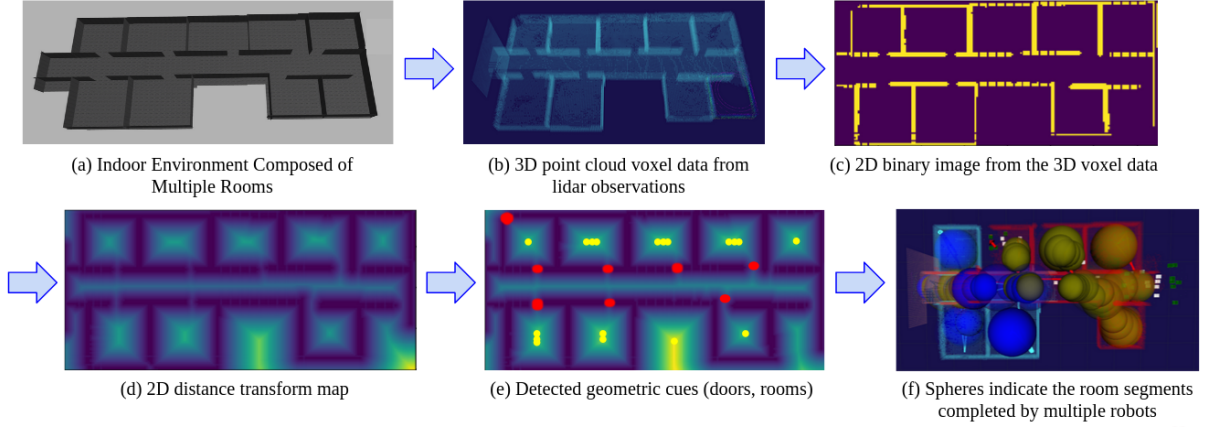


Fig. 2. Overview of our exploration pipeline. (a): The robot is exploring an indoor environment composed of multiple rooms. (b): It processes 3D point cloud voxel data observed from LiDAR sensors. (c),(d),(e): 3D point clouds turn into 2D binary image, then into 2D distance transform map, which the robot uses to detect the geometric cues like doors and rooms. (f): Each open space like room is represented as a sphere or a set of spheres in our pipeline; blue spheres are the spaces that are explored by the robot (self) and yellow spheres are the spaces that are explored by other robots.

rooms that are observed by the primary sensor of robot i is

$$\left| \bigcup_{j=1, \dots, K} (O_i \cap V_j^{\text{rm}}) \right| \quad (1)$$

($|\cdot|$ is the number of voxels). In this work, we will reward robots for exploring rooms in a building rather than increasing total coverage by traversing corridors and hallways.

In the multi-robot setting, our objective is to maximize the union of such voxels, explored by all robots collectively. Each robot finds its own trajectory ξ_i seeking to maximize the union of observed voxels in rooms by all robots,

$$\xi_1^*, \xi_2^*, \dots, \xi_n^* = \arg \max_{\xi_1, \xi_2, \dots, \xi_n} \left| \bigcup_{i=1..n} \left(\bigcup_{j=1..K} (O_i \cap V_j^{\text{rm}}) \right) \right| \quad (2)$$

given a fixed time. The robots will solve (2) approximately and in a decentralized manner, so that each robot will plan its own path ξ_i^* while communicating with other robots.

IV. DISTRIBUTED EXPLORATION METHOD

In this section, we present our autonomous distributed exploration pipeline, which coordinates the behaviors of multiple robots exploring in a building composed of multiple rooms. The pipeline overview is displayed in Fig. 2. We first explain preliminary background on the autonomous robot exploration baseline [10], which we build upon and improve (Sec. IV-A). Then, we describe the two main building blocks of our method, geometric cue extraction (Sec. IV-B, Alg. 1) and spherical decomposition of space (Sec. IV-C, Alg. 2). We also explain the multi-robot communication and target assignment (Sec. IV-D, Alg. 3), and finally explain how they all come together to form our Multi-Robot Multi-Room (MRMR) method (Sec. IV-E, Alg. 4).

A. Preliminary: Autonomous Exploration Baseline

The baseline method we use is the open source autonomous aerial robot exploration pipeline [10] developed by Team Explorer, to compete in DARPA Subterranean Challenge. This baseline enables robots to navigate in a wide

range of challenging underground or indoor environments such as a mine, subway, tunnel, or cave, with limited communication, sensor coverage, and light conditions.

The baseline method leverages LiDAR sensors to discover the geometry of surrounding environments, using OpenVDB [29] as a data structure for representing map occupancy grids, and SLAM solutions generated by Super Odometry [30].

The path planning component of the baseline method, which we focus on in this work, can be loosely categorized as a frontier-based exploration approach with graph search and selection heuristics. Using vision and range sensors, the robot generates a set of *viewpoints* at the frontiers. The viewpoints are scored with heuristics, and the viewpoints with high scores are selected. Then, paths are planned to reach the viewpoints. RRT-Connect [31] is used to find a feasible global path to viewpoints, and A* graph search and motion primitives are used for local path planning.

For multi-robot exploration, onboard communication hardware is used, and the plans for robots are coordinated implicitly by sharing knowledge of the world. This includes knowing the take-off locations of each robot, and communicated shared map in a global reference frame.

B. Extracting Geometric Cues of Doors and Rooms

The first component of our method is detection of doors and rooms via geometric cue extraction, as shown in Alg. 1. The intuition for this algorithm is that *saddle points* on the distance transform are approximately equivalent to the locations of doors. We also extract local maxima to approximate locations of centers of open spaces such as rooms.

The robot incrementally obtains 3D point cloud observations from onboard sensors which it uses to maintain a voxel grid map. The 3D point cloud map voxels O are flattened into 2D binary map B , by taking all occupied voxels within the range of height $z \in [z_{\text{low}}, z_{\text{high}}]$. In practice, we set $z_{\text{low}} = 0$ and $z_{\text{high}} = 1.8$. Any obstacles like walls are represented as 1, and any free spaces like narrow passageways or corridors are represented as 0, in this binary map.

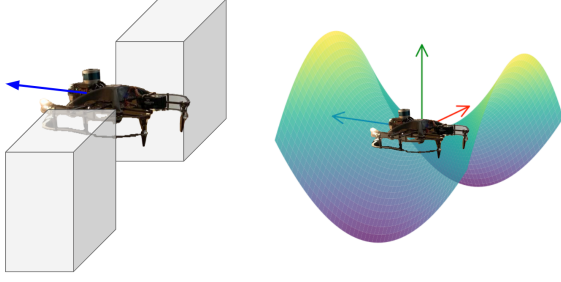


Fig. 3. Our geometric cue extraction method detects saddle points that correspond to the potential location of doors. In terms of distance to wall, the door is at its relative maximum along the axis of wall, but is at its relative minimum along the crossing axis of free voxels.

Algorithm 1 ExtractCues

Input: 3D Point Cloud Map Voxel Grid Data O

- 1: Create 2D binary map B by taking $z \in [z_{\text{low}}, z_{\text{high}}]$
- 2: Get distance map $M = \text{distanceTransform}(\text{filter}(B))$
- 3: Compute Hessian matrix $H \leftarrow \text{Hessian}(M)$
- 4: Obtain a set of saddle points (doors) P^{sadd} from H
- 5: Obtain a set of local maxima (center) P^{max} from H
- 6: For each $c \in P^{\text{max}}$, obtain distance δ between c to the closest wall using distance map M . This set is Δ

Output: P^{sadd} as potential doors, (P^{max}, Δ) as potential center locations of rooms and minimum distances to wall

Then the robot converts the binary map B into distance transform map M , which computes the minimal distance to closest occupied pixel for all pixels. Then the robot obtains a second-order partial derivative matrix of the distance map, or hessian H , from which it can compute saddle points P^{sadd} and local maxima P^{max} , using the determinant¹:

$$\det(x, y) = f_{xx}(x, y)f_{yy}(x, y) - (f_{xy}(x, y))^2, \quad (3)$$

and with P^{sadd} and P^{max} defined as

$$\begin{cases} (x, y) \in P^{\text{sadd}} & \text{if } \det(x, y) < -0.1 \\ (x, y) \in P^{\text{max}} & \text{if } \det(x, y) > 0 \ \& \ f_{xx}(x, y) < -0.1 \end{cases} \quad (4)$$

A local maximum $c \in P^{\text{max}}$ is a point, whose distance $\delta \in \Delta$ to the wall is the highest compared to other neighboring pixels. In practice, these points correspond to the center points of spaces surrounded by walls, such as rooms.

The more interesting part is the use of saddle points (visualized in Fig. 3). A saddle point refers to a critical point that is not a local extremum; any points that are a relative minimum along one axis and relative maximum along another perpendicular axis are classified as saddle points. In our setting, doors are detected as saddle points: a door point is at its relative maximum in terms of distance to a wall along the wall-axis (the voxels occupied by walls have

¹For second-order derivative test, we empirically found that detecting points that meet the condition $\det(x, y) < -0.1$ (instead of $\det(x, y) < 0$) works well in practice to find saddle points. Similarly, we set $f_{xx}(x, y) < -0.1$ as a threshold for detecting local maxima.

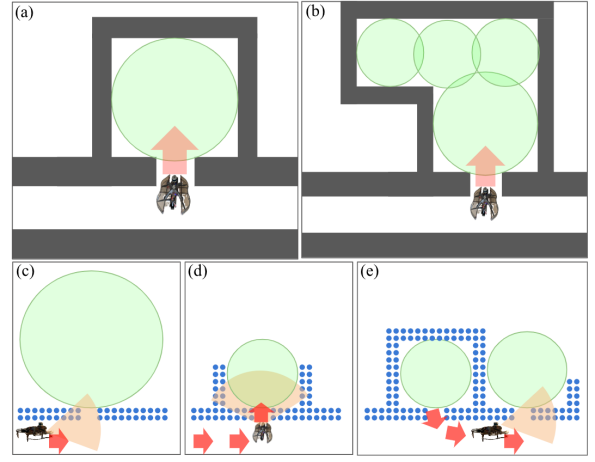


Fig. 4. A room is represented (a) by a sphere, or (b) by a set of spheres. Commanding robot to reach to the center of the sphere(s) is sufficient for obtaining full information of the room. The size and location of spheres are adjusted as the robot collects more 3D voxel grid data, as in (c),(d),(e)

zero distance to the walls); the door point is at its relative minimum along the crossing axis, which is composed of free voxels that lie perpendicular to the walls, that have higher distance to wall than door.

C. Spherical Decomposition of Space

We make a design choice to represent the space by decomposing it into a set of spheres. A sphere is defined by the (x, y, z) coordinates of the center and a radius. The output of Alg. 1 includes pairs of local maximum and its distance to the wall; by taking each pair of local maximum and its distance from the wall, we can generate spheres of center at $c \in P^{\text{max}}$ and radius of $\delta \in \Delta$.

We argue that this is a compact representation of the world, in the context of room exploration. A typical square-shaped room, as shown in Fig. 4(a), can be represented by using a single sphere, whose center is located in the middle of the room and the sphere's boundary is adjoining to the walls of the room (as the radius is distance from the center to the closest wall). Other types of rooms, for example, a concave room like Fig. 4(b) can be composed into multiple convex parts and represented by a set of spheres.

Why do we use spheres as representation for spaces like rooms? First, it is efficient for robot's room exploration. In order for a robot to cover the space and observe information around 360° surroundings, it suffices to command the robot to reach to the center of the sphere; at the center of the sphere, the robot can observe a large area surrounded by the wall, as the center is the local maximum on the distance transform and radius is its distance to occupied space. Second, it is an efficient data structure (just center and radius) to be shared among robots under limited communication. This will be explained in the Sec. IV-D.

The spherical decomposition of the space is not static, as the robot updates the map of the environment by incrementally obtaining more information of the surrounding (e.g. discovers a new wall). An exemplary scenario is Fig. 4

Algorithm 2 UpdateSpheres

Input: A pre-existing set of spheres S (previous spherical decomposition of space), a set of pair of local maxima and distance (P^{\max}, Δ) from the output of Alg. 1

```
1: for each  $(c, \delta)$  pair do  $\triangleright c \in P^{\max}, \delta \in \Delta$ 
2:   generate a sphere  $s$  of center  $c$  and radius  $\delta$ 
3:   for each pre-existing sphere  $s' \in S$  do
4:      $r_1$  and  $r_2 \leftarrow$  radius of  $s$  and  $s'$ 
5:      $d \leftarrow$  distance between centers of  $s$  and  $s'$ 
6:     if  $d < 0.5(r_1 + r_2)$ :  $\triangleright$  if spheres are too close
7:       choose / save the larger one between  $s$  and  $s'$ 
8:     elif  $d < (r_1 + r_2)$ :  $\triangleright$  if medium-distanced
9:       merge the spheres by weighted-average them
10:    end for
11:    if  $s$  isn't merged to any pre-existing  $s' \in S$ :
12:      simply add  $s$  to  $S$ 
13: end for
Output:  $S$ 
```

(c),(d),(e): When the robot moves straight along the corridor, the geometry beyond the wall is unknown, so it assumes that there is a large open space, as in Fig. 4(c). When observations are made through the door into the room, a partial map of the room is formed. As in Fig. 4(d), the robot updates the sphere so that it adjoins the walls. In Fig. 4(e), the robot has finished exploring the first room, and starts collecting data on the right side of the first room, adjusting the size and location of a new sphere accordingly.

While rooms are represented by spheres, they are not equivalent with rooms; in fact, any free space between walls or surrounded by walls can be represented by spheres. For instance, corridors are also filled with spheres. In practice, their existence doesn't affect the algorithm, as the target sphere is chosen after a door is reached. (See Sec. IV-E)

Algorithm 2 is a process of maintaining and updating a set of spheres, when new inputs (pairs of local maxima and distance to the wall) are continuously fed into the system. If the new sphere is closely located to any of the pre-existing spheres, it is merged into one of them; otherwise, it is simply added to the spherical decomposition set.

D. Multi-Robot Communication and Target Assignment

As discussed in Sec. IV-B, the robot extracts geometric cues and detects saddle points as potential doors, and it also represents rooms with spherical decomposition of spaces as discussed in Sec. IV-C. For distributed target assignment among multiple robots, we utilize the doors and spheres as information to be shared. Each robot maintains a set of doors D_r and a set of spheres S_r it has reached based on its local map; these two sets are also shared with other robots via communication. Sets of doors (lists of points in 3D coordinates) and sets of spheres (lists of points and radii) serve as a compact representation of the explored space. Each robot then maintains a set of doors D_o and spheres S_o reached by other robots alongside the local sets (D_r, S_r).

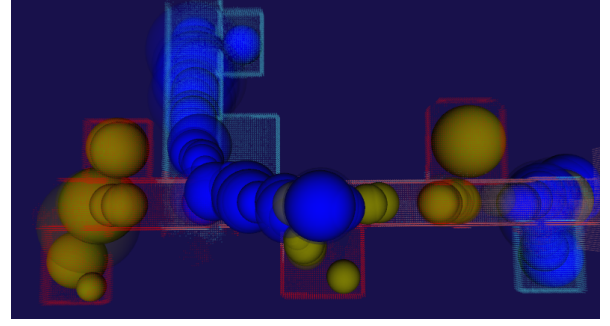


Fig. 5. Example image of spherical decomposition of space for distributed target assignments. The spheres that were reached by the first and second robot are colored blue and yellow, respectively.

Algorithm 3 TargetAssignmentAndCommunication

Input: Set of spheres and doors robot reached S_r, D_r , set of spheres and doors other robots reached S_o, D_o , threshold parameters $\epsilon_d = 1.0$ and $\epsilon_s = 1.5$

```
1: Targeting a new door:
2:   given a set of candidate doors  $D$ , exclude the doors that were already reached, thus  $D \leftarrow D \setminus D_r$ 
3:   for each  $d \in D$ :
4:     if  $\exists d' \in D_o$  such that  $\text{dist}(d, d') < \epsilon_d$ :
5:       exclude this  $d$ , thus  $D \leftarrow D \setminus \{d\}$ 
6:   choose the closest  $d \in D$  as a new target door
7: Targeting a new sphere:
8:   given a set of candidate spheres  $S$ , exclude the spheres that were already reached, thus  $S \leftarrow S \setminus S_r$ 
9:   for each  $s \in S$ :
10:    if  $\exists s' \in S_o$  such that  $\text{dist}(s.\text{center}, s'.\text{center}) < \epsilon_s$ :
11:      exclude this  $s$ , thus  $S \leftarrow S \setminus \{s\}$ 
12:   choose the closest  $s \in S$  as a new target sphere
13: Inter-Robot Communication:
14:   robot publishes spheres  $S_r$  and doors  $D_r$  it reached
15:   robot subscribes to other robots' published  $S_r, D_r$  and save them to  $S_o$  and  $D_o$ 
```

When targeting a new door, the robot not only excludes doors reached by itself but also doors reached by other robots. Any candidate door d that is distanced less than ϵ_d from any of the doors reached by other robots D_o is excluded. Likewise, robots exclude both spheres they have reached along with spheres reached by other robots when targeting a new sphere. The details of this distributed target assignment scheme are explained in Alg. 3. This algorithm runs on each robot, without any centralized planner.

E. Multi-Robot Multi-Room (MRMR) Exploration

Here, we explain how the previous algorithms come together and fit into one method, Multi-Robot Multi-Room (MRMR) exploration. The detailed procedure is in Alg. 4. At every timestep, the robot extracts geometric cues, detecting saddle points, local maxima, and distances to the walls, and updates the spherical decomposition of the space. Then the robot targets a door, reaches the door, and explores a room by targeting a sphere or a set of the spheres that constitute

Algorithm 4 Multi-robot Multi-room (MRMR) exploration. Algorithm is run on each robot.

Input: robot R , initialize observed_map O , spheres S with empty sets $\{\}$, initialize S_r, D_r, S_o, D_o (as defined in Alg 3) with empty sets $\{\}$

- 1: **for** each timestep **do**
- 2: \triangleright *geometric analysis of observed map:*
- 3: $P^{\text{sadd}}, (P^{\text{max}}, \Delta) \leftarrow \text{ExtractCues}(O)$ \triangleright Alg 1
- 4: $S \leftarrow \text{UpdateSpheres}(S, (P^{\text{max}}, \Delta))$ \triangleright Alg 2
- 5: \triangleright *door finding:*
- 6: **if** R is not targeting any door:
- 7: target closest door $d \in P^{\text{sadd}}$ \triangleright Alg 3
- 8: generate path to d and execute
- 9: **if** R reached the target door:
- 10: $D_r \leftarrow D_r \cup \{d\}$ \triangleright mark this door as reached
- 11: \triangleright *room exploration:*
- 12: target closest sphere $s \in S$ \triangleright Alg 3
- 13: generate and execute path to $s.\text{center}$
- 14: **if** the room is composed of multiple spheres:
- 15: **while** spheres remaining in the room:
- 16: target next adjacent sphere s \triangleright Alg 3
- 17: generate path to $s.\text{center}$ and execute
- 18: **for** each sphere s that was reached:
- 19: $S_r \leftarrow S_r \cup \{s\}$ \triangleright mark spheres as reached
- 20: \triangleright *multi-robot communication:*
- 21: update S_o, D_o via communication \triangleright Alg 3
- 22: \triangleright *no-target phase:*
- 23: **if** there is no door or room to target:
- 24: run baseline [10] until finding next door
- 25: **end for**

Output: Path trajectory traveled by R

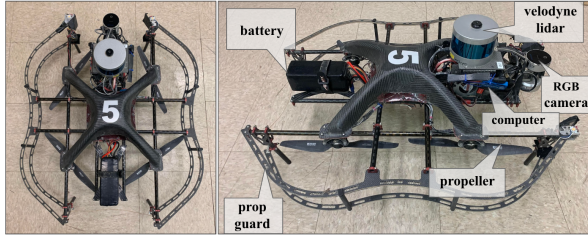


Fig. 6. Aerial robot system hardware. Left: top-view, Right: side-view. Custom-built quadrotor robot equipped with sensors and computer onboard.

the room. Whenever the robot reaches a door and a center of the sphere, these are marked as *reached*, so that it can avoid re-targeting the doors or rooms that were already explored. This information is also shared with other robots, which are concurrently running the algorithm; each robot shares what it has already reached and what other robots have already reached which enables effective distributed target assignment. Lastly, when there is no door or room to explore, the robot runs a frontier-based RRT-exploration baseline [10] until it finds the next geometric cues from observations.

TABLE I
THE DETAILS OF THE SIMULATION TEST ENVIRONMENTS.

Name	Images	Rooms	Volume (m^3)	Voxels
Env1		6	462.6	9587
Env2		8	776.7	21313
Env3		5	402.9	11869
Env4		9	729.1	20105
Env5		12	1179.1	33371

TABLE II
THE SUMMARY OF SIMULATION EXPERIMENTS

Method	1 Robot		2 Robots		3 Robots	
	Voxels	Rooms	Voxels	Rooms	Voxels	Rooms
Baseline	26.72%	17.36%	40.46%	39.28%	51.29%	53.95%
MRMR	36.73%	39.63%	59.28%	48.95%	64.51%	60.68%
Improvement	37.46%	128.28%	46.51%	24.62%	25.77%	12.47%

V. EXPERIMENTS & RESULTS

In this section, we explain the experimental setup and display results to evaluate our algorithm, MRMR. We first elaborate on the experimental setup and discuss results for simulation environments. Then we discuss the experimental setup and results for real-robot experiments. For comparison, we chose the previous frontier-based exploration [10] as a baseline, both in simulation and real-robot experiments.

A. Simulation Experiments

1) *Experimental Setup:* We used the SubT UAV code released by [10], developed to simulate real subterranean environments. We designed five new indoor simulation environments with different configurations and numbers of rooms, and Table I illustrates the floorplan, number of rooms, volume of the total room spaces (in m^3), and number of grid voxels in rooms of each environment. We tested with different numbers of robots ($n = 1, 2, 3$) and measured the number of union of observed voxels in the rooms by the robots collectively with their primary sensor cameras over time (max time = 2 minutes). Each graph curve is an average of three independent runs. We also measured percentages of voxels in rooms observed (out of total voxels in rooms) and number of rooms (out of total number of rooms) by each method, and displayed the results in a separate table.

2) *Results:* The results of the simulation experiments are displayed in Fig. 7. The plots in the first row of the figure are single-robot case, and the plots in the second and third row

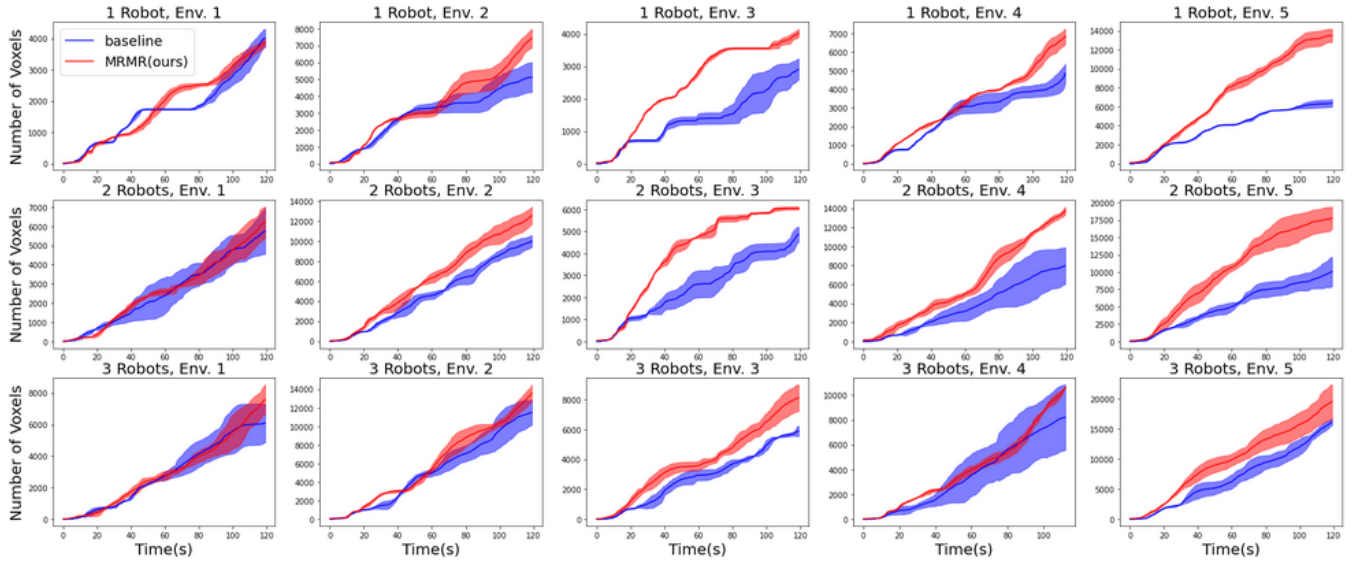


Fig. 7. The comparison of baseline and our method (MRMR). The first, second, third row is 1-robot, 2-robots, and 3-robots case respectively, and each column represents each different environment. Results show that our MRMR method observes more voxels in rooms than the baseline.

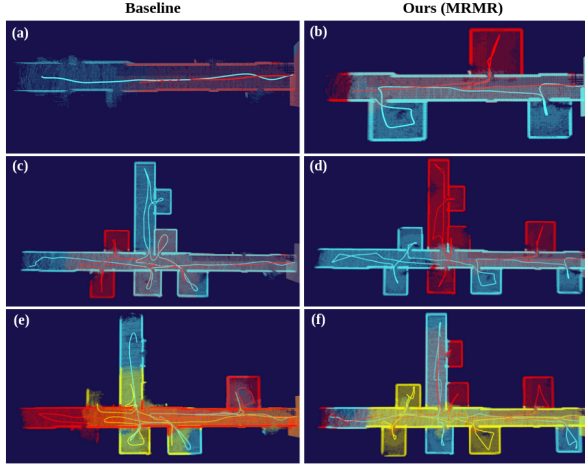


Fig. 8. Visualization of baseline’s and our method’s behaviors. (a) Using the baseline, the robots travel the corridor first by moving straight, while (b) using our method, robots quickly turn directions to find doors and enter the rooms. (c),(e): multiple robots often enter the same rooms redundantly. (d),(f): each room is uniquely visited by each robot using our method.

are multi-robot cases (2-robots and 3-robots). These plots demonstrate that our Method (MRMR) observes more voxels in the rooms than frontier-based baseline, across different environments and different number of robots. In average, MRMR observes 37.46%, 46.51%, 25.77% more room grid voxels than baseline in single-robot, two-robot, and three-robot cases. In the Table II, we reported how MRMR method observes more voxels (out of total room voxels) and explore more rooms (out of total number of rooms) than baseline; MRMR outperforms the baseline both in terms of voxels observed and number of rooms explored.

More qualitative explanations of difference between the baseline and MRMR are following: as shown in Fig. 8(a), using the baseline, robots first choose to travel corridors fast

TABLE III

THE SUMMARY OF REAL-ROBOT EXPERIMENTS OVER THREE TRIALS

#	2 Robots				3 Robots			
	Baseline Vxl.	Rm.	MRMR Vxl.	Rm.	Baseline Vxl.	Rm.	MRMR Vxl.	Rm.
1.	6204	3	10285	5	11584	5	15732	8
2.	10721	5	9428	5	14336	7	17320	9
3.	8437	4	11724	6	14561	7	15976	8

by moving straight to increase the coverage area without turning to the doors or rooms. In contrary, as in Fig. 8(b), the robots quickly turn directions to reach the doors and enter rooms, rather than simply increasing coverage. Using the baseline (Fig. 8(c),(e)), multiple robots often enter the same rooms redundantly and sometimes miss exploring rooms; in contrary our method (Fig. 8(d),(f)) enables robots to uniquely visit each room without redundancy.

B. Real-Robot Experiments

1) *Experimental Setup*: For real-world experiments, we use custom quadrotors as shown in Fig. 6. Each drone is 68cm wide, 81cm long, weighs 5.2kg, and is equipped with a Velodyne VLP-16 Lidar, Realsense RGBD sensors, Intel NUC computer with Intel Core i7-8550U CPU. We run experiments in an abandoned hospital in Pittsburgh, PA. The main results compare our method to the baseline with two to three robots; drones fly sequentially as the mechanism for inter-robot collision avoidance for real robots is limited. *Additionally*, we report results of a trial with three robots flying *simultaneously* with our method only. We report the number of voxels in rooms, as well as number of rooms collectively observed by the robots for both experiments.

2) *Results*: The results of the real-robot experiments are displayed in the Table III. In the comparative tests, both in

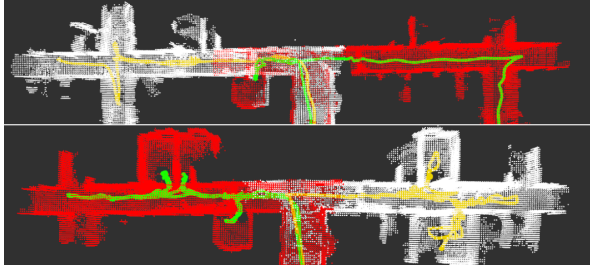


Fig. 9. The comparison of area covered and trajectory traveled between baseline (upper) vs MRMR (lower) in real-robot experiments (two-robot case). MRMR observes more rooms than baseline.

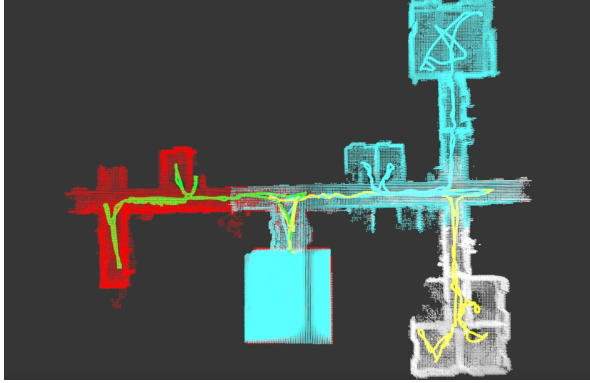


Fig. 10. Three robots are *simultaneously* exploring rooms in real-drone experiments; the trajectory and area covered by each robot is visualized with different color.

two-robot and three-robot cases, the robots generally observe more grid voxels and explore more rooms using MRMR. The exception is trial 2 of the two-robot case where the baseline outperforms MRMR but by an insignificant amount. On average, MRMR observes 30.66%, 22.09% more grid voxels in rooms than the baseline, in two-robot and three-robot cases respectively. Additionally, Fig. 9 visualizes the results of running both methods with two robots. Finally, in the simultaneous execution experiment (Fig. 10), the robots successfully explored 8 rooms using MRMR, observing 16793 voxels in the rooms, with three drones.

VI. CONCLUSION & FUTURE WORK

We proposed a multi-robot multi-room autonomous exploration pipeline (MRMR) that methodically explores and performs detailed observations of rooms in a building and coordinates behaviors of robot teams. To this end, we presented a geometric cue extraction method that detects locations of doors and rooms from point clouds, and spherical decomposition of open spaces for target assignment. We validated performance of our method in simulated and real experiments. Some limitations are that the approach is only applicable to single story buildings due to flattening of 3D voxels into a 2D distance transform map, and that the collision avoidance among aerial robots is implicit, rather than explicit. For future work, we plan to extend our approach to multi-floor buildings and to consider exploration with heterogeneous multi-robot systems and to improve such systems with advanced vision and learning modules.

REFERENCES

- [1] W. Burgard, M. Moors, C. Stachniss, and F. E. Schneider, "Coordinated Multi-Robot Exploration," *IEEE Trans. Robotics*, vol. 21, no. 3, pp. 376–386, 2005.
- [2] J. Braga, A. P. Aguiar, and J. B. de Sousa, "Coordinated Multi-UAV Exploration Strategy for Large Areas with Communication Constraints," in *ROBOT 2017: Third Iberian Robotics Conference: Volume 1*, 2017, pp. 149–160.
- [3] J. P. Queralta *et al.*, "Collaborative Multi-Robot Search and Rescue: Planning, Coordination, Perception, and Active Vision," *IEEE Access*, 2020.
- [4] B. Ristic *et al.*, "Autonomous Multi-Robot Search for a Hazardous Source in a Turbulent Environment," *Sensors*, vol. 17, no. 4, p. 918, 2017.
- [5] M. J. Schuster *et al.*, "Towards Autonomous Planetary Exploration," *Journal of Intelligent & Robotic Systems*, vol. 93, pp. 461–494, 2019.
- [6] M. Kulkarni *et al.*, "Autonomous Teamed Exploration of Subterranean Environments using Legged and Aerial Robots," in *2022 International Conference on Robotics and Automation (ICRA)*, 2022, pp. 3306–3313.
- [7] S. Scherer *et al.*, "Resilient and Modular Subterranean Exploration with a Team of Roving and Flying Robots," *Field Robotics Journal*, pp. 678–734, May 2022.
- [8] A. Agha, K. Otsu, B. Morrell, D. D. Fan, R. Thakker *et al.*, "Nebula: Quest for Robotic Autonomy in Challenging Environments; TEAM CoSTAR at the DARPA Subterranean Challenge," *arXiv preprint arXiv:2103.11470*, 2021.
- [9] B. Yamauchi, "Frontier-Based Exploration using Multiple Robots," in *The 2nd International Conference on Autonomous Agents*, 1998, pp. 47–53.
- [10] G. Best, R. Garg, J. Keller, G. A. Hollinger, and S. Scherer, "Resilient Multi-Sensor Exploration of Multifarious Environments with a Team of Aerial Robots," in *Proceedings of Robotics: Science and Systems*, 2022.
- [11] G. A. Hollinger and G. S. Sukhatme, "Sampling-based Motion Planning for Robotic Information Gathering," in *Robotics: Science and Systems*, 2013.
- [12] B. Charrow, *Information-Theoretic Active Perception for Multi-Robot Teams*. University of Pennsylvania, 2015.
- [13] M. Corah and N. Michael, "Distributed Matroid-Constrained Submodular Maximization for Multi-Robot Exploration: Theory and Practice," *Autonomous Robots*, vol. 43, pp. 485–501, 2019.
- [14] T. Dang, M. Tranzatto, S. Khattak, F. Mascariach, K. Alexis, and M. Hutter, "Graph-based Subterranean Exploration Path Planning using Aerial and Legged Robots," *Journal of Field Robotics*, vol. 37, no. 8, pp. 1363–1388, 2020.
- [15] Y. Sung and P. Tokekar, "A Competitive Algorithm for Online Multi-Robot Exploration of a Translating Plume," in *International Conference on Robotics and Automation, ICRA*, 2019, pp. 3391–3397.
- [16] J. Yan, X. Lin, Z. Ren, S. Zhao, J. Yu, C. Cao, P. Yin, J. Zhang, and S. A. Scherer, "MUL-TARE: Multi-Agent Cooperative Exploration with Unknown Initial Position," *CoRR*, vol. abs/2209.10775, 2022.
- [17] R. Luna and K. E. Bekris, "Efficient and Complete Centralized Multi-Robot Path Planning," in *IEEE/RSJ International Conference on Intelligent Robots and Systems*, 2011, pp. 3268–3275.
- [18] F. Gul, A. Mir, I. Mir, S. Mir, T. U. Islaam, L. Abualigah, and A. Forestiero, "A Centralized Strategy for Multi-Agent Exploration," *IEEE Access*, vol. 10, pp. 126 871–126 884, 2022.
- [19] Q. Li, F. Gama, A. Ribeiro, and A. Prorok, "Graph Neural Networks for Decentralized Multi-Robot Path Planning," in *IEEE/RSJ International Conference on Intelligent Robots and Systems*, 2020, pp. 11 785–11 792.
- [20] Y. Zhai, B. Ding, X. Liu, H. Jia, Y. Zhao, and J. Luo, "Decentralized Multi-Robot Collision Avoidance in Complex Scenarios with Selective Communication," *IEEE Robotics and Automation Letters*, vol. 6, no. 4, pp. 8379–8386, 2021.
- [21] L. Wu *et al.*, "Voronoi-based Space Partitioning for Coordinated Multi-Robot Exploration," *Journal of Physical Agents*, 2007.
- [22] A. Solanas and M. Garcia, "Coordinated Multi-Robot Exploration through Unsupervised Clustering of Unknown Space," in *IEEE/RSJ International Conference on Intelligent Robots and Systems*, 2004.
- [23] J. Hu, H. Niu, J. Carrasco, B. Lennox, and F. Arvin, "Voronoi-based Multi-Robot Autonomous Exploration in Unknown Environments via Deep Reinforcement Learning," *IEEE Trans. Veh. Technol.*, vol. 69, no. 12, pp. 14 413–14 423, 2020.
- [24] S. Thrun, "Learning Metric-Topological Maps for Indoor Mobile Robot Navigation," *Artificial Intelligence*, vol. 99, no. 1, pp. 21–71, 1998.
- [25] K. M. Wurm, C. Stachniss, and W. Burgard, "Coordinated Multi-Robot Exploration using a Segmentation of the Environment," in *IEEE/RSJ International Conference on Intelligent Robots and Systems*, 2008, pp. 1160–1165.
- [26] E. Brunskill, T. Kollar, and N. Roy, "Topological Mapping using Spectral Clustering and Classification," in *IEEE/RSJ International Conference on Intelligent Robots and Systems*, 2007, pp. 3491–3496.
- [27] K. Sjöö, "Semantic Map Segmentation using Function-based Energy Maximization," in *IEEE International Conference on Robotics and Automation*, 2012, pp. 4066–4073.
- [28] A. Rosinol, A. Gupta, M. Abate, J. Shi, and L. Carlone, "3D Dynamic Scene Graphs: Actionable Spatial Perception with Places, Objects, and Humans," in *Robotics: Science and Systems XVI*, 2020.
- [29] K. Museth, "VDB: High-Resolution Sparse Volumes with Dynamic Topology," *ACM transactions on graphics (TOG)*, vol. 32, no. 3, pp. 1–22, 2013.
- [30] S. Zhao *et al.*, "Super Odometry: IMU-centric LiDAR-Visual-Inertial Estimator for Challenging Environments," in *IEEE/RSJ International Conference on Intelligent Robots and Systems*, 2021, pp. 8729–8736.
- [31] J. J. Kuffner and S. M. LaValle, "RRT-Connect: An Efficient Approach to Single-Query Path Planning," in *Proceedings of IEEE International Conference on Robotics and Automation*, vol. 2, 2000, pp. 995–1001.